Chemical Physics Letters 590 (2013) 92–96

Contents lists available at ScienceDirect

Chemical Physics Letters

journal homepage: www.elsevier.com/locate/cplett

CuO reduction induced formation of CuO/Cu_2O hybrid oxides

Lu Yuan [a], Qiyue Yin [a], Yiqian Wang [b], Guangwen Zhou [a,*]

[a] Department of Mechanical Engineering & Multidisciplinary Program in Materials Science and Engineering, State University of New York, Binghamton, NY 13902, United States
[b] The Cultivation Base for State Key Laboratory, Qingdao University, Qingdao 266071, China

ARTICLE INFO

Article history:
Received 7 September 2013
In final form 15 October 2013
Available online 22 October 2013

ABSTRACT

Reduction of CuO nanowires results in the formation of a unique hierarchical hybrid nanostructure, in which the parent oxide phase (CuO) works as the skeleton while the lower oxide (Cu_2O) resulting from the reduction reaction forms as partially embedded nanoparticles that decorate the skeleton of the parent oxide. Using *in situ* transmission electron microscopy observations of the reduction process of CuO nanowires, we demonstrate that the formation of such a hierarchical hybrid oxide structure is induced by topotactic nucleation and growth of Cu_2O islands on the parent CuO nanowires.

1. Introduction

Transitional metal oxides consist of a large family of materials exhibiting a variety of interesting properties [1,2]. One of the characteristics of transitional metal oxides is their ability to adopt multiple oxidation states. The ease with which the different oxidation states of transitional metal oxides can be interconverted has led to their wide usages in batteries [3], catalysts [4], photoelectrochemical devices [5], sensors [6], etc. The reduction of transitional metal oxides represents an important class of heterogeneous reactions that allows for the interconversion of various metal oxidation states with various coordination environments and heterogeneous interfaces. It is generally believed that the reaction commences with the nucleation of a reduced phase (an oxide phase with a lower oxidation state) at localized sites of the parent oxide, followed by the growth of these nuclei at the expense of the parent phase as lattice oxygen is removed from the parent oxide phase [7,8]. However, the nucleation and growth process of the oxide reduction is still largely unexplored because many of the oxide systems of interest were studied in the bulk.

The nanowire morphology presents a highly oriented one-dimensional skeleton and it is of fundamental and technological interest to understand how oxide-reduction induced phase transformations take place within one-dimensional systems. Using oxide nanowires as a platform, herein we show the oxide reduction results in the formation of a hierarchical structure of hybrid oxides consisting of the parent nanowire stem and partially embedded nanoparticles with a different oxidation state. A hybrid nanostructure consisting of nanowires and nanoparticles combines the intrinsic merits of the inherently high specific surface area of nanoparticles and the anisotropic properties of nanowires [9–11]. The formation of such hierarchical hybrid materials can allow for multifunctional properties and applications that are not available with just the individual components or a single phase.

Among many metal oxides, the reduction of copper oxides is an important reference system and has been the subject of extensive studies for understanding the reaction mechanism and reaction pathways between the different oxidation states (Cu^{2+} vs. Cu^{1+}) and oxide crystal structures (Cu_2O cubic vs. CuO monoclinic) [7,12–20]. By examining the reduction of CuO nanowires, we show the formation of a hierarchical nanostructure of hybrid oxides composed of CuO nanowire stem and Cu_2O nanoparticles that partially embed into the parent CuO nanowires. Using *in situ* transmission electron microscopy (TEM) observations of the oxide reduction process, we further demonstrate that the formation of such a hybrid oxide structure is related to the oxide–reduction induced nucleation and growth of Cu_2O nanoparticles on the parent CuO nanowires.

2. Experimental

Our approach involves a two-step process (oxidation and reduction) as schematically illustrated in Figure 1a. At first, CuO nanowires can be prepared by heating a Cu foil (polycrystalline Cu foils, 99.99% purity, obtained from Sigma–Aldrich) in air [21] or in a vacuum chamber filled with oxygen gas [22–26]. In our experiment, the Cu substrate was oxidized for 2 h at 450 °C and 200 Torr of oxygen pressure to grow CuO nanowires. This procedure yields well-aligned CuO nanowires perpendicular to the metal substrate (CuO nanowires are grown on both surfaces of the oxidized Cu foil). To study the oxide reduction, the oxidized Cu samples were directly annealed at 450 °C for different durations (1–4 h) in the same chamber under the vacuum of $\sim 2 \times 10^{-6}$ Torr and then cooled down in the vacuum to room temperature. *In situ* TEM observations of the oxide reduction process were also performed using a Gatan TEM heating holder within a JEOL JEM2100F microscope operated at 200 kV. CuO nano-

* Corresponding author. Fax: +1 6077774620.
E-mail address: gzhou@binghamton.edu (G. Zhou).

0009-2614/$ - see front matter © 2013 Elsevier B.V. All rights reserved.
http://dx.doi.org/10.1016/j.cplett.2013.10.040

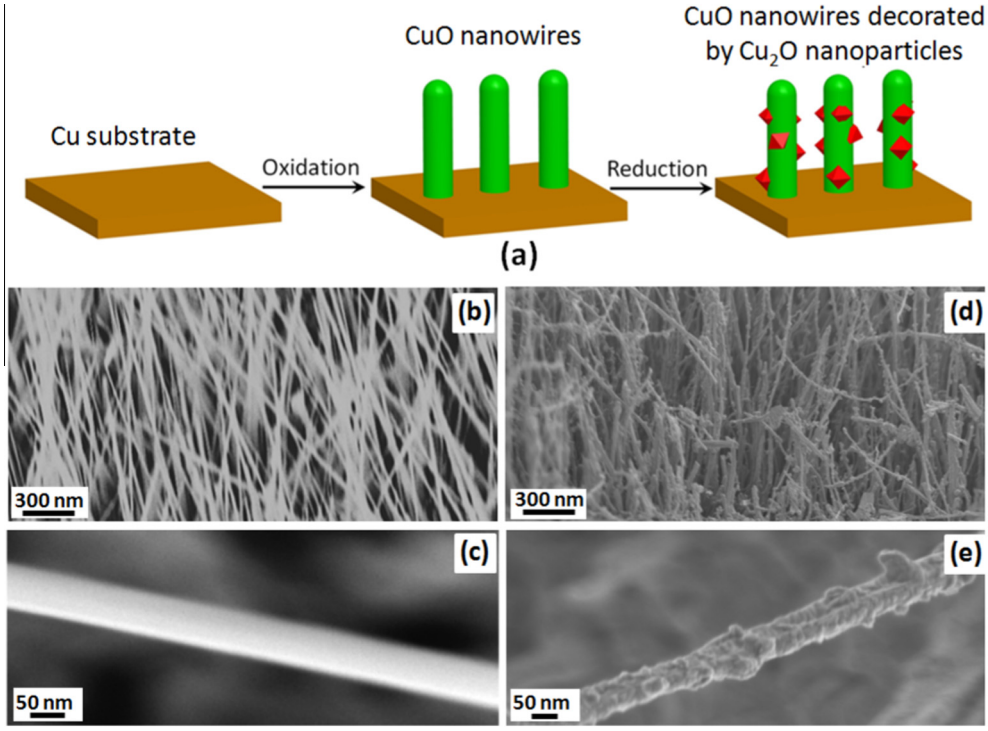

Figure 1. (a) Schematic illustration of the combined oxidation–reduction reactions employed to generate oxide hybrid oxides; (b) SEM image of CuO nanowires formed from the oxidation of a Cu substrate; (c) zoom-in SEM image revealing the smooth surface and straight morphology of individual CuO nanowires; (d) SEM image of CuO nanowires being reduced under vacuum at 400 °C for 2 h; (e) zoom-in SEM image showing that the surface of reduced CuO nanowires is covered by tiny particles.

wires used for the *in situ* TEM experiments were collected from the oxidized Cu substrates. The TEM samples were plasma cleaned before the *in situ* TEM heating experiments.

3. Results and Discussion

Figure 1b shows a representative scanning electron microscopy (SEM) image of CuO nanowires formed from the oxidation of a Cu substrate. The CuO nanowires have lengths up to several microns and relatively uniform diameter (~100 nm) along the axial direction. Figure 1c presents a zoom-in SEM image of a single CuO nanowire, showing that the nanowires have smooth surfaces. Figure 1d shows a typical SEM image of CuO nanowires after being annealed under vacuum at 450 °C for 2 h. The initially straight and smooth nanowires become a little curved with significantly increased surface roughness. Some of the reduced nanowires show saw-toothed surface morphology. As revealed by a zoom-in SEM image shown in Figure 1e, the nanowire surface is covered by a high density of nanoparticles.

The density of nanoparticles formed on the CuO nanowires depends on the reduction time. Figure 2a shows a representative TEM image of CuO nanowires reduced by the vacuum annealing at 450 °C for 1 h. Compared to Figure 1d, e, the surface density of nanoparticles on the CuO nanowire is decreased due to the short reduction time. The crystal structures of the nanowire and nanoparticles are determined by electron diffraction. Figure 2b is an electron micro-diffraction pattern recorded from the dashed circle region of the nanowire shown in Figure 2a, which matches well with the crystal structure of single crystal CuO with the $[1\bar{1}2]$ zone axis. Figure 2c is an electron diffraction obtained from the nanoparticle as indicated in the inset TEM image zoomed in from the dashed rectangular region in Figure 2a, which can be indexed well with the Cu_2O structure along the $[0\bar{1}1]$ zone axis. Figure 2d is an SAED pattern obtained from the nanoparticle–nanowire overlapping region and two sets of diffraction patterns, one from the parent CuO nanowire and the other from the Cu_2O nanoparticle, are visible. The orientation relation between the Cu_2O nanoparticle and the parent CuO nanowire can be identified from the diffraction patterns, $[1\bar{1}2]$ CuO//$[0\bar{1}1]$ Cu_2O, i.e., the reduction of the CuO phase occurs via topotactic nucleation and growth of Cu_2O islands on the parent CuO nanowire.

The microstructure of the reduced nanowires is further characterized by high-resolution TEM (HRTEM). Figure 3a shows a TEM image of an individual CuO nanowire before the reduction reaction, where a bi-crystal twin boundary (TB) is present along the length direction. This is further confirmed by the HRTEM image as shown in Figure 3b, which reveals that each side of the nanowire is single crystal with well-defined lattice structure. The axial direction of the nanowire is along $\langle 2\bar{1}0 \rangle$ as identified from the selected area electron diffraction shown in the inset of Figure 3a. Figure 3c displays a TEM image of a CuO nanowire reduced by vacuum annealing at 450 °C for 1 h, which shows clearly the formation of Cu_2O islands on the parent CuO nanowire. The growth morphology revealed by the TEM observation suggests that the Cu_2O islands nucleate on the outer surface of the CuO nanowires and grow into the nanowire by consuming the CuO phase. Figure 3d is a HRTEM image from the Cu_2O/CuO interface area as indicated by a dashed square in Figure 3c. The Cu_2O/CuO interface formed from the oxide reduction is clearly visible, where the bi-crystal boundary present in the original CuO nanowire still remains intact and serves as a marker to differentiate from the unreacted region of the CuO nanowire in addition to the different crystal lattice structures of the two oxide phases. Figure 3d also shows that the CuO lattice contrast becomes slightly blurred near the CuO/Cu_2O interface, which may be caused by the increased lattice distortion due to the lattice mismatch between the two oxides. The thickness difference at the Cu_2O/CuO interface may also contribute to the blurred lattice contrast due to the different TEM focus distance.

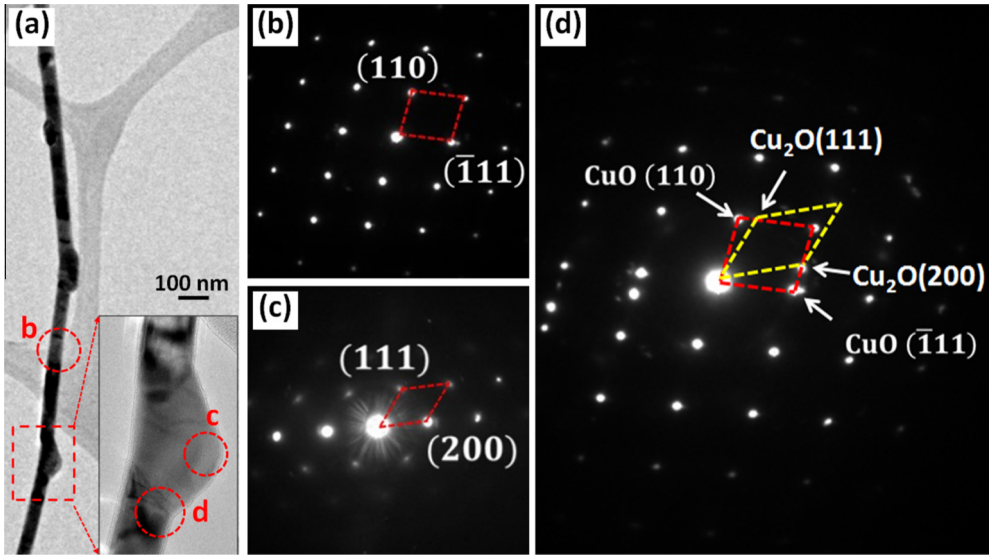

Figure 2. (a) TEM image of CuO nanowires reduced under vacuum for 1 h; (b) SAED pattern obtained from the parent nanowire indicated by the dashed circle in (a); (c) SAED pattern from the nanoparticle marked by the dashed circle shown in the inset zoomed-in TEM image of (a); (d) SAED pattern from the nanoparticle–nanowire overlapping region marked by the dashed circle as shown in the inset zoomed-in image of (a).

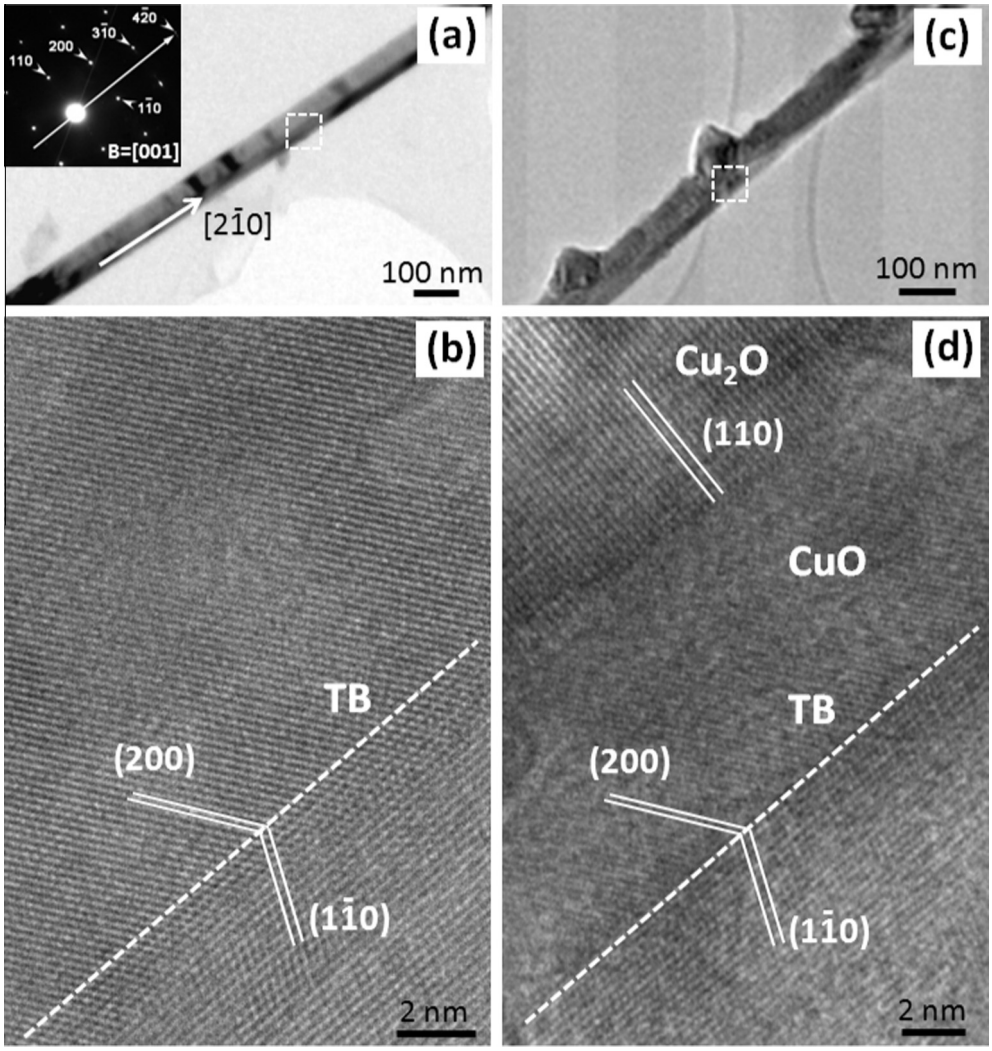

Figure 3. (a) TEM image of a single CuO nanowire, (b) HRTEM image obtained from the region marked by dashed white square in (a), inset is a selected area electron diffraction pattern revealing that the axial direction of the nanowire is along ⟨ 2$\bar{1}$0 ⟩; (c) TEM image of a reduced CuO nanowire, showing the formation of Cu_2O nanoparticles; (d) HRTEM image obtained from the region indicated by the dashed white square in (c).

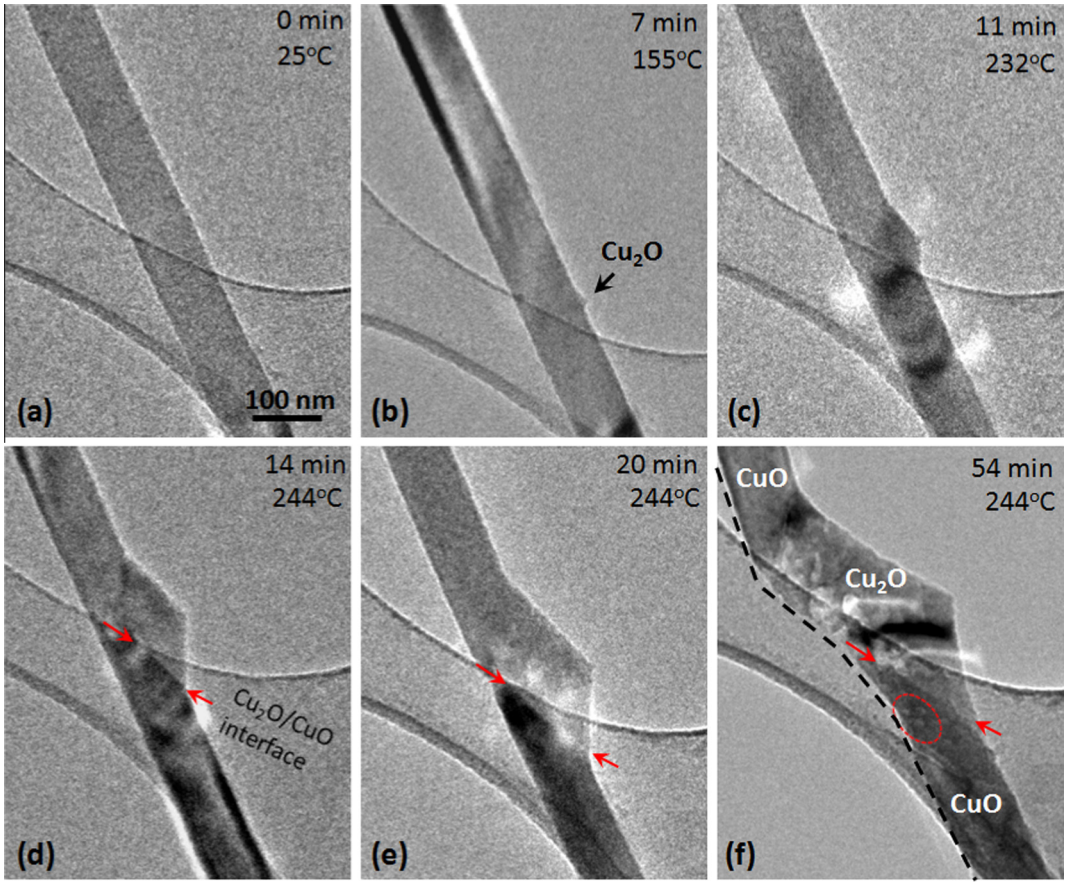

Figure 4. Time-resolved *in situ* TEM images taken dynamically to reveal the nucleation and growth of a Cu_2O island on the surface of a CuO nanowire during the CuO reduction process as the temperature ramps up from room temperature to 244 °C under the TEM column vacuum. The red arrows in (d, e, f) indicate the position of the Cu_2O/CuO interface. Pores (in the region marked by a dashed red circle in (f)) are formed in the CuO nanowire during the reduction. The dashed black line in (f) marks the formation of a kink after the Cu_2O island completely penetrates through the CuO nanowire. (For interpretation of the references to colour in this figure legend, the reader is referred to the web version of this article.)

In situ TEM observations were also employed to monitor the oxide reduction induced phase and morphological evolution. The nucleation and growth of Cu_2O nanoparticles during the reduction of a CuO nanowire was observed in real time. Figure 4 shows a time-lapsed series of *in situ* TEM images of the reduction of a single CuO nanowire, where the sample was gradually heated from room temperature to ~240 °C under the vacuum of $\sim 10^{-6}$ Torr (i.e., the vacuum in the sample region of the TEM column). As seen in Figure 4a, the CuO nanowire is straight and has a uniform diameter and smooth surface before the reduction transformation. After the temperature was increased to ~155 °C, a Cu_2O nucleus becomes visible (Figure 4b), and *in situ* TEM imaging reveals that the Cu_2O island nucleates on the surface of the CuO nanowire and grows three dimensionally into the CuO nanowire. To enhance the reduction kinetics, the sample temperature was further increased to ~244 °C and then held at this temperature. With the continued annealing, the Cu_2O island grows further into the CuO nanowire, resulting in a double pyramid shape of the Cu_2O island with a wedge-shaped Cu_2O/CuO interface, as seen in Figure 4d. The pairs of arrows in Figure 4d–f mark the position and its propagation of the Cu_2O/CuO interface during the reaction. The *in situ* TEM images show that the double-pyramid shape of the Cu_2O island was retained until the Cu_2O island completely penetrates through the nanowire along the diameter direction (Figure 4f).

It can be seen that the overall nanowire morphology (straight and uniform diameter) during the oxide reduction can be retained before the Cu_2O island penetrates through the nanowire. This suggests that the CuO → Cu_2O transition is localized at the Cu_2O/CuO interface. However, Cu and O atoms supplying the phase transformation is not limited to the Cu_2O/CuO interface region only, i.e., Cu and O atoms diffuse from other regions of the CuO nanowire to the Cu_2O/CuO interface for the CuO disproportionation reaction CuO (solid) → Cu_2O (solid) + 1/2 O_2 (gas). This can be evidenced from observed small pores (e.g., marked by a dashed red circle in Figure 4f) in the CuO regions away from the Cu_2O/CuO interface. The reduction of the parent oxide is accompanied with the removal of lattice oxygen, which leaves behind oxygen vacancies and un-coordinated Cu atoms that diffuse to the Cu_2O/CuO interface for Cu_2O growth. The continued CuO reduction results in the increased concentration of O and Cu vacancies that eventually coalescence to form pores in the CuO nanowire. As indicated by the dashed black line in Figure 4f, the penetration of the Cu_2O island through the CuO nanowire induces significant morphology change from the initially straight nanowire to a kinked nanowire with the Cu_2O island inserted at the kinked location. Our *in situ* TEM observations indicate that the shape of the nanowire can be completely lost due to the formation of pores and Cu_2O island growth with increasing the reduction time.

Thermochemically, CuO is unstable under the condition of low oxygen pressure and high temperatures [27]. The reduction of bulk CuO via the disproportionation reaction CuO → Cu_2O + 1/2 O_2 takes place typically above 800 °C upon vacuum annealing [28]. However, our experimental observations shown above indicate that the reduction of CuO nanowires begins at ~150 °C (i.e., see Figure 4b). Such a significantly lower temperature may suggest a size

effect of the nanowire morphology, where a large fraction of atoms are located in a close proximity to the surface and thus conducive to the phase transformation at a significantly lower reaction temperature. This is consistent with the *in situ* TEM observations, which revealed that the nucleation of the Cu_2O phase indeed initiates at the outer surface of the nanowire (Figure 4b). Our observations also corroborate previous surface science studies, which showed that the reduction of CuO surface region during the vacuum annealing begins at a considerably lower temperature to form a surface layer of Cu_2O by monitoring the chemical states of Cu and O [29–31].

4. Conclusion

In summary, we have shown that the oxide–reduction induced phase transformation in one-dimensional oxide nanowires results in the formation of a novel hierarchical nanostructure that combines the oxides with different oxidation states. This is demonstrated by the reduction of CuO nanowires that leads to the formation of a hybrid structure of Cu_2O–CuO oxides, where the parent CuO nanowires serve as the skeleton and the lower oxide of the Cu_2O phase resulting from the CuO reduction forms as nanoparticles on the parent CuO nanowires. The mechanism underlying the formation of these hybrid oxides is identified as the topotactic nucleation and growth of the lower oxide on the parent oxide. By carefully choosing the reduction conditions such as temperature, reducing gases, and the form (e.g. particles, thin films) of the oxides, we expect our results are more general and have broader applicability for developing novel hybrid structures.

Acknowledgements

This work was supported by the National Science Foundation under NSF CAREER Award Grant CMMI-1056611. Y.Q. Wang would like to thank the financial support from the Natural Science Foundation for Outstanding Young Scientists in Shandong Province, China (Grant no.: JQ201002).

References

[1] M. Fernandez-Garcia, A. Martinez-Arias, J.C. Hanson, J.A. Rodriguez, Chem. Rev. 104 (2004) 4063.
[2] F.P. Netzer, J. Vac. Sci. Technol. B 28 (2010) 1.
[3] M.S. Whittingham, Chem. Rev. 104 (2004) 4271.
[4] H.H. Kung, Transition Metal Oxides: Surface Chemistry and Catalysis, Elsevier, New York, 1989.
[5] K. Kalyanasundaram, M. Gratzal, Coord. Chem. Rev. 77 (1998) 347.
[6] G. Korotcenkov, Mater. Sci. Eng., B 139 (2007) 1.
[7] J.A. Rodriguez, J.C. Hanson, A.I. Frenkel, J.Y. Kim, M. Perez, J. Am. Chem. Soc. 124 (2002) 346.
[8] C.H. Bamford, C.F.H. Tipper, R.G. Compton, Reactions of solids with gases, vol. 21, Elsevier, New York, 1984.
[9] Y. Xia et al., Adv. Mater. 15 (2003) 353.
[10] X. Wang, X. Sun, J. Xu, Y. Li, in: Z.L. Wang (Ed), Nanowires and Nanobelts: Materials, Properties, and Devices, vol. 2, Springer, New York, 2003, p. 173.
[11] Y.Z. Feng, I.S. Cho, P.M. Rao, L.L. Cai, X.L. Zheng, Nano Lett. 13 (2013) 855.
[12] J.Y. Kim, J.A. Rodriguez, J.C. Hanson, A.I. Frenkel, P.L. Lee, J. Am. Chem. Soc. 125 (2003) 10684.
[13] J. Pike, S.W. Chan, F. Zhang, X.Q. Wang, J. Hanson, Appl. Catal., A 303 (2006) 273.
[14] J.A. Rodriguez, J.Y. Kim, J.C. Hanson, M. Perez, A.I. Frenkel, Catal. Lett. 85 (2003) 247.
[15] X.Q. Wang, J.C. Hanson, A.I. Frenkel, J.Y. Kim, J.A. Rodrigues, J. Phys. Chem. B 108 (2004) 13667.
[16] G.W. Zhou, J.C. Yang, Phys. Rev. Lett. 93 (2004) 226101.
[17] G.W. Zhou, W.Y. Dai, J.C. Yang, Phys. Rev. B 77 (2008) 245427.
[18] Y. Qin, S.M. Lee, A.L. Pan, U. Gosele, M. Knez, Nano Lett. 8 (2008) 114.
[19] J. Li, J.W. Mayer, K.N. Tu, Phys. Rev. B 45 (1992) 5683.
[20] L. Li, G.W. Zhou, Surf. Sci. 605 (2011) 54.
[21] X.C. Jiang, T. Herricks, Y.N. Xia, Nano Lett. 2 (2002) 1333.
[22] L. Yuan, Y.Q. Wang, R. Mema, G.W. Zhou, Acta Mater. 59 (2011) 2491.
[23] L. Yuan, G.W. Zhou, J. Electrochem. Soc. 159 (2012) C205.
[24] L. Yuan, Q.K. Jiang, J.B. Wang, G.W. Zhou, J. Mater. Res. 27 (2012) 1014.
[25] L. Yuan, Y.Q. Wang, R.S. Cai, Q.K. Jiang, J.B. Wang, B.Q. Li, G.W. Zhou, Mater. Sci. Eng., B 177 (2012) 327.
[26] R. Mema, L. Yuan, Q. Du, Y. Wang, G.W. Zhou, Chem. Phys. Lett. 512 (2011) 87.
[27] D.V. Ragone, Thermodynamics of Materials, Wiley, New York, 1995.
[28] F.A. Cotton, G. Wilkinson, Advanced Inorganic Chemistry, Wiley, Chichester, 1988. p. 768.
[29] G.G. Jernigan, G.A. Somorjai, J. Catal. 147 (1994) 567.
[30] S. Poulston, P.M. Parlett, P. Stone, M. Bowker, Surf. Interface Anal. 24 (1996) 811.
[31] S.Y. Lee, N. Mettlach, N. Ngugen, Y.M. Sun, J.M. White, Appl. Surf. Sci. 206 (2003) 102.